GENETICS

Complete enzyme set for chlorophyll biosynthesis in *Escherichia coli*

Guangyu E. Chen,[1] Daniel P. Canniffe,[1]* Samuel F. H. Barnett,[1] Sarah Hollingshead,[1]† Amanda A. Brindley,[1] Cvetelin Vasilev,[1] Donald A. Bryant,[2] C. Neil Hunter[1]‡

Chlorophylls are essential cofactors for photosynthesis, which sustains global food chains and oxygen production. Billions of tons of chlorophylls are synthesized annually, yet full understanding of chlorophyll biosynthesis has been hindered by the lack of characterization of the Mg–protoporphyrin IX monomethyl ester oxidative cyclase step, which confers the distinctive green color of these pigments. We demonstrate cyclase activity using heterologously expressed enzyme. Next, we assemble a genetic module that encodes the complete chlorophyll biosynthetic pathway and show that it functions in *Escherichia coli*. Expression of 12 genes converts endogenous protoporphyrin IX into chlorophyll a, turning *E. coli* cells green. Our results delineate a minimum set of enzymes required to make chlorophyll and establish a platform for engineering photosynthesis in a heterotrophic model organism.

INTRODUCTION

Chlorophylls (Chls) underpin photosynthesis, which generates the oxygen that supports all complex life on Earth and the reducing potential to fix carbon dioxide as carbohydrates, the ultimate source of all the organic compounds required for life on Earth. The annual production of Chls, on land and in the oceans, is on the scale of billions of tons, yet the enzyme components of the biosynthesis pathway have neither been fully determined nor assembled to define the minimal set of genes required to make Chl. The Chl biosynthetic pathway (Fig. 1A) is a branch of tetrapyrrole biosynthesis, and it begins with protoporphyrin IX (PPIX), which is also the precursor for heme biosynthesis. Most life forms, including those able to photosynthesize, make PPIX and convert it to heme by inserting Fe^{2+} into the porphyrin macrocycle. Heme is a cofactor for respiratory proteins, and it is also converted into bilins, linear tetrapyrroles that are used as light-harvesting pigments in cyanobacteria.

Chl biosynthesis is initiated when the magnesium chelatase enzyme complex (ChlIDH, Gun4) inserts Mg^{2+} into PPIX, so the Mg^{2+}/Fe^{2+} Chl/heme branchpoint in photosynthetic bacteria, algae, and plants requires fine control to ensure that the correct amounts of hemes, bilins, and Chls are produced (*1*). Following the production of Mg-PPIX (MgP), six more enzymatic steps culminate in the production of Chl a, the ubiquitous pigment of oxygenic photosynthesis (see Fig. 1A). The MgP methyltransferase (ChlM) produces the substrate for the MgP monomethyl ester (MgPME) cyclase (AcsF), which produces 3,8-divinyl protochlorophyllide a (DV PChlide a); this intermediate has acquired a fifth ring that imparts the green color characteristic of Chls. Protochlorophyllide oxidoreductase (POR) produces 3,8-divinyl chlorophyllide a (DV Chlide a), which is reduced by divinyl reductase (DVR) and then esterified with geranylgeranyl pyrophosphate (GGPP) by Chl synthase (ChlG) to produce GG–Chl a. Finally, the reduction of the GG "tail," catalyzed by GG reductase (ChlP), completes the pathway, and Chl a is produced. At this point, the pigment is hydrophobic and enters the membrane-bound assembly pathway for photosynthetic complexes, where it engages with the Sec/YidC-assembly machinery that coordinates the cotranslational insertion of nascent photosystem polypeptides with pigment production (*2*). Many steps of the Chl biosynthesis pathway have been studied individually in mutant strains of phototrophs, and some of the early steps have been characterized to define kinetic parameters (*3*), but it is not known whether these enzymes are sufficient to assemble the pathway and convert PPIX to Chl a. Apart from the global significance of Chl biosynthesis, the bottom-up construction of this pathway represents the first step in reprogramming a heterotrophic bacterium for growth under a variety of predetermined conditions of light intensity and wavelength. This metabolic engineering, which would also require genes encoding photosynthetic apoproteins, not only addresses important biological problems such as the concept of the minimal amount of genetic information required for photosynthetic life but also lays the groundwork for engineering cell factories with light-powered metabolism.

RESULTS AND DISCUSSION

In vivo cyclase activity of heterologously expressed AcsF

From the outset, the major obstacle for constructing a complete Chl biosynthetic pathway was the cyclase step, the activity of which has never been demonstrated using a recombinant enzyme. There are two mechanistically unrelated cyclases: an oxygen-sensitive, radical-SAM enzyme with a [4Fe-4S] cluster encoded by the *bchE* gene in most anoxygenic phototrophic bacteria (*4*) and an oxygen-dependent di-iron enzyme in some purple proteobacteria, as well as cyanobacteria, algae, and higher plants (*5*). We previously delineated three distinct classes of the oxygen-dependent cyclase in terms of subunit composition (*5*); one class comprises only one known subunit, AcsF, and the other two cyclases require an additional subunit, either BciE or Ycf54, for activity. Studies on barley mutants (*6*) indicated that additional subunits were required to form an active cyclase complex, and substantial effort had been made to identify a missing component. To verify that AcsF is the sole cyclase component, we transferred the *acsF* gene (*7*) from one purple bacterial phototroph, *Rubrivivax* (*Rvi.*) *gelatinosus*, to another that lacks the oxygen-dependent cyclase, *Rhodobacter* (*Rba.*) *capsulatus*. The *bchE* gene encoding the oxygen-sensitive cyclase was then deleted from the recipient (fig. S1A), as was the *ccoP* gene encoding a subunit of the

[1]Department of Molecular Biology and Biotechnology, University of Sheffield, Firth Court, Western Bank, Sheffield S10 2TN, UK. [2]Department of Biochemistry and Molecular Biology, Pennsylvania State University, University Park, PA 16802, USA.
*Present address: Department of Biochemistry and Molecular Biology, Pennsylvania State University, University Park, PA 16802, USA.
†Present address: Sir William Dunn School of Pathology, University of Oxford, Oxford OX4 2DY, UK.
‡Corresponding author. Email: c.n.hunter@sheffield.ac.uk

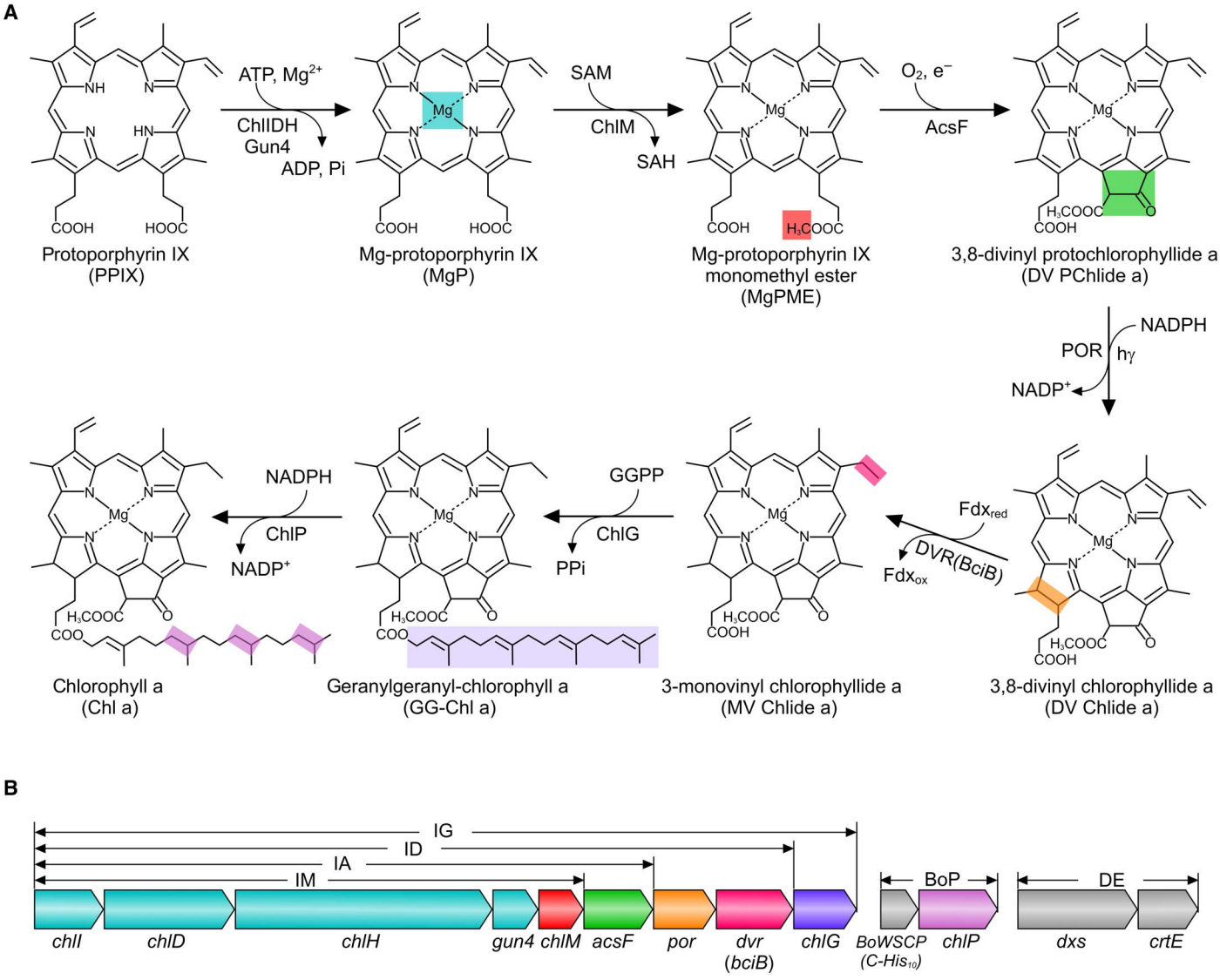

Fig. 1. Assembly of the Chl biosynthesis pathway in *Escherichia coli*. (**A**) Overall reactions from PPIX to Chl a catalyzed by the enzymes introduced to *E. coli*. The insertion of Fe^{2+} into PPIX (not shown) creates a biosynthetic branchpoint (not shown) that yields heme. Colored shading denotes the chemical change(s) at each step. ATP, adenosine triphosphate; ADP, adenosine diphosphate; SAM, *S*-adenosine-L-methionine; SAH, *S*-adenosyl-L-homocysteine; $NADP^+$, nicotinamide adenine dinucleotide phosphate; NADPH, reduced form of $NADP^+$; Pi, inorganic phosphate; PPi, inorganic pyrophosphate. (**B**) Arrangement and relative size of each gene in the constructed plasmids. The *chlI*, *chlD*, *chlH*, *gun4*, *chlM*, *acsF*, *dvr* (*bciB*), and *chlG* genes were consecutively cloned into a modified pET3a vector with a single T7 promoter upstream of *chlI* and a ribosome-binding site upstream of each gene using the link-and-lock method (see fig. S2 for details) (*40*). Colors for genes correspond to those used in (A). Plasmid constructs and gene contents are IM (*chlI–chlM*), IA (*chlI–acsF*), ID (*chlI–dvr*), IG (*chlI–chlG*), BoP (*BoWSCP* and *chlP*), and DE (*dxs* and *crtE*). BoP is a pACYCDuet1-based plasmid containing a sequence encoding the BoWSCP protein with a C-terminal His_{10} tag (*10*) and the *Synechocystis chlP* gene. DE is a pCOLADuet1-based plasmid containing the *E. coli dxs* gene and the *Rvi. gelatinosus crtE* gene.

oxygen scavenging cbb_3 oxidase in *Rba. capsulatus* (fig. S1B). This latter manipulation should increase the intracellular oxygen concentration and allow the foreign AcsF cyclase to function (*8*). Bacteriochlorophyll biosynthesis and assembly of photosynthetic complexes were abolished in the Δ*bchE*Δ*ccoP* mutant, which, when harboring the pBB[*acsF*] plasmid-containing *Rvi. gelatinosus acsF*, regained nearly wild-type levels of pigmentation (Fig. 2, A and B).

To demonstrate AcsF activity in a nonphotosynthetic bacterium, we conducted an in vivo cyclase assay with an *E. coli* strain expressing the *Rvi. gelatinosus acsF* gene. *E. coli* cultures were fed MgPME, the cyclase substrate, which can diffuse across the lipid bilayer of *E. coli* membranes because of its hydrophobic nature; analysis of pigments by high-performance liquid chromatography (HPLC) showed that DV PChlide a, the product of the cyclase, was detected in the strain expressing *acsF* and was absent in the control strain (Fig. 2C). The in vivo conversion of MgPME into DV PChlide a in *E. coli* confirms that the *Rvi. gelatinosus* AcsF alone is a functional cyclase, requiring no additional subunit for activity; thus, it is a highly suitable candidate for assembling a Chl biosynthesis pathway in a heterotrophic bacterium, using the minimum number of components.

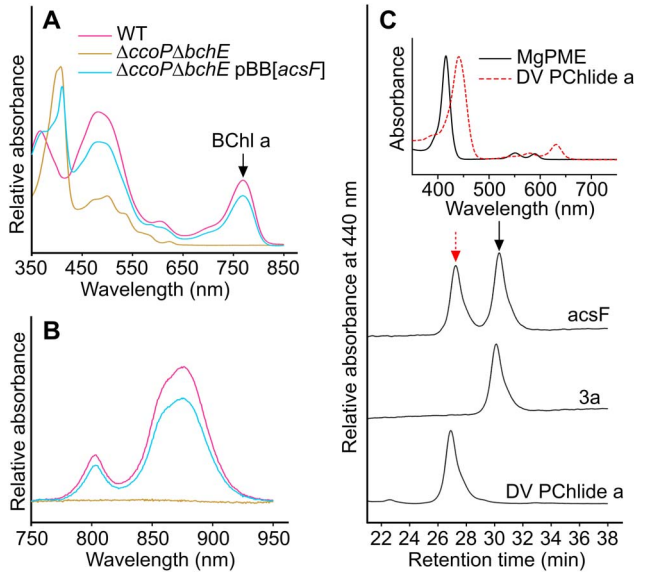

Fig. 2. In vivo cyclase activity of heterologously expressed AcsF. (**A** and **B**) The cyclase activity is linked to the (A) production of bacteriochlorophyll a (BChl a) and (B) assembly of photosynthetic complexes in *Rba. capsulatus*. (**C**) HPLC analysis of pigment methanol extracts from in vivo cyclase assays conducted with *E. coli* strains harboring either the pET3a (3a) or pET3a-*acsF* (acsF) plasmid. *E. coli* cultures were grown to an optical density at 600 nm (OD_{600}) of 0.4 to 0.6 and then induced with isopropyl-β-D-thiogalactopyranoside (IPTG) and incubated with MgPME.

Assembly of the Chl biosynthesis pathway in *E. coli*

After demonstrating the in vivo cyclase activity of the *Rvi. gelatinosus* AcsF, we tested the known components of Chl biosynthesis by engineering the whole pathway (Fig. 1A) in the nonpigmented enteric bacterium *E. coli*. Genes encoding enzymes that mediate the six enzymatic steps of the Chl biosynthesis pathway were assembled into one operon (Fig. 1B), starting from the conversion of PPIX to MgP. We used the genes for Chl biosynthesis from the cyanobacterium *Synechocystis* sp. PCC 6803 (hereafter referred to as *Synechocystis*), except for the cyclase-encoding gene *acsF*, which was from *Rvi. gelatinosus*. The *Rvi. gelatinosus crtE* gene, encoding the GGPP synthase, was also included to modify the nonmevalonate pathway in *E. coli* to produce GGPP, a substrate for Chl synthase. To ensure sufficient isopentenyl PP for GGPP production, we overexpressed the native *E. coli dxs* gene, encoding one of the rate-limiting steps of the nonmevalonate pathway (*9*). A sequence encoding the *Brassica oleracea* (var. *gemmifera*) water-soluble Chl protein (BoWSCP) (*10*) was included, in an attempt to sequester the hydrophobic and phototoxic Chl molecules produced by this engineered pathway. All genes used are listed in table S1. The progressively larger constructs depicted in Fig. 1B represent an increasingly complete pathway and contain genes from *chlI* to *chlM*, then to *acsF*, to *dvr*, and finally to *chlG*; they were named IM, IA, ID, and IG, respectively. In addition, the *Synechocystis* cyclase-encoding genes *cycI* and *ycf54* were cloned into the IM plasmid, resulting in the IM-*cycI-ycf54* construct (fig. S3).

The *E. coli* C43(DE3) strain (*11*), a strain effective for expression of toxic proteins, was used as the host. Single transformations of *E. coli* C43 (DE3) yielded the IM, IA, ID, IG, and IM-*cycI-ycf54* strains; two and three sequential transformations were conducted to obtain the DE/IG and DE/BoP/IG strains, respectively. The resulting strains were assayed for their capacities to synthesize Chl intermediates at various stages and the final product, Chl a (see Materials and Methods). Pigments were extracted from the harvested *E. coli* cells using methanol and analyzed by HPLC with elution profiles monitored by absorbance at 416, 440, and 665 nm (Fig. 3, B to E; see figs. S3 to S5 for additional controls).

Control strain 3a, containing the empty pET3a vector, did not accumulate any Chl intermediates (Fig. 3). MgPME was produced in the IM strain (Fig. 3B), and the IA strain accumulated DV PChlide a (Fig. 3C), as did the IM-*cycI-ycf54* strain containing the *cycI and ycf54* genes (*12*–*15*) from the cyanobacterium *Synechocystis* (fig. S3). On the basis of retention times and positions of Soret absorption bands, the pigments in the ID strain were identified as monovinyl (MV) PChlide a and MV Chlide a (Fig. 3D). The trace level of MV Chlide a in the dark sample was likely produced by unavoidable light exposure during experimental procedures. The increased level of MV Chlide a and substantial decrease in MV PChlide a upon light treatment demonstrate that the ID strain harbors an active light-dependent POR enzyme and show that we have built a biosynthetic pathway that converts PPIX to MV Chlide a. Further biosynthetic steps (Fig. 3E) do not alter the absorption properties of the pigment, so HPLC was used to assess the completion of the pathway, which relies on the availability of GGPP to esterify MV Chlide a. The IG strain accumulated a new pigment (retention time, 46.9 min; Fig. 3E), which is much more hydrophobic than MV Chlide a (retention time, 20.2 min) and likely to be Chl a esterified with a farnesyl moiety; the immediate precursor of GGPP, farnesyl PP, is produced in *E. coli*, and Chl synthase has been reported to be able to use farnesyl PP as a substrate (*16*). The combination of the DE and IG plasmids enables *E. coli* to produce GG–Chl a. Three successive reductions of the GG tail, catalyzed by the GG reductase ChlP, complete the Chl pathway. The noticeable green color of the DE/BoP/IG strain and identification of Chl a by HPLC and liquid chromatography–mass spectrometry (LC-MS; Fig. 3E and fig. S6) demonstrate the successful assembly of the Chl biosynthetic pathway in *E. coli*. We estimate that the productivity of Chl a in the DE/BoP/IG strain under the tested conditions was ~1000 molecules per cell, equivalent to a concentration of ~1 μM in *E. coli* cells.

Finally, the pigmentation of the engineered *E. coli* cells was imaged at the single-cell level by structured illumination microscopy (SIM) (*17*) and fluorescence spectroscopy. Figure 4A demonstrates that newly synthesized Chl a molecules are exclusively localized in the native cytoplasmic membrane [with an in vivo emission maximum at 676 nm (Fig. 4H)] rather than in the cytosolic recombinant BoWSCP (see fig. S7 for immunodetection of the protein), a natural scavenger of Chls (*18*). In plants, cyanobacteria, and algae, the destination of Chls is a series of transmembrane multisubunit complexes, the assembly pathways of which are under active investigation in many laboratories (*19*–*21*). BoWSCP was included here because it represents a relatively simple, cytosolic target for binding newly synthesized Chls. Previously, we have shown that the phototrophic bacterium *Rba. sphaeroides*, which normally makes bacteriochlorophyll, can be engineered to synthesize Chl a, which was subsequently assembled in vivo into the BoWSCP (*10*). Although this protein is synthesized by *E. coli* (fig. S7), evidence for Chl binding was inconclusive because of the low levels of BoWSCP synthesized. The factors that determine in vivo assembly of Chl into water-soluble and membrane-bound complexes in *E. coli* require further study.

Concluding remarks

This research completes our understanding of how the tetrapyrrole pigments of life, namely, siroheme (*22*), hemes (*23*, *24*), bilins (*25*, *26*), vitamin B_{12} (*27*), coenzyme F_{430} (*28*, *29*), and now Chls, are synthesized from a common template. By identifying the elusive oxidative ring

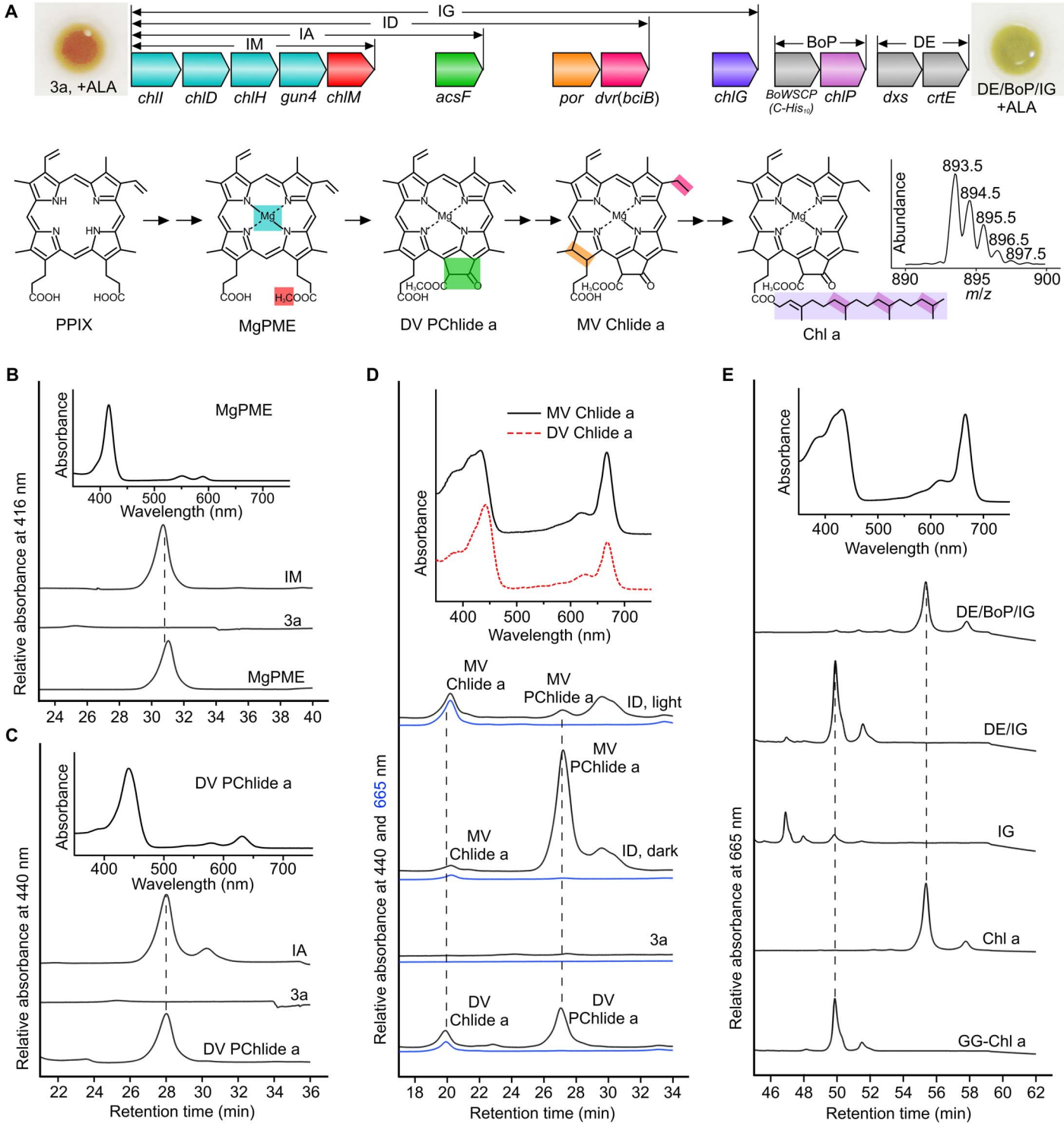

Fig. 3. Pigment accumulation in *E. coli* strains expressing Chl biosynthesis genes. (**A**) Photographs of cell pellets of the *E. coli* control strain accumulating PPIX (3a) and the Chl a–producing strain (DE/BoP/IG) grown with supplementation of δ-aminolevulinic acid (ALA). Pigment production in described *E. coli* strains was analyzed by HPLC. *m/z*, mass/charge ratio. (**B**) Accumulation of MgPME in the IM strain monitored by absorbance at 416 nm. (**C**) Accumulation of DV PChlide a in the IA strain monitored by absorbance at 440 nm. (**D**) Light-dependent production of MV Chlide a in the ID strain monitored by absorbance at 440 nm (shown in black) and 665 nm (shown in blue). POR was activated by treatment with 5 μmol photons m^{-2} s^{-1} light at the latter stage of the incubation. The small MV Chlide a peak detected in the dark sample is due to unavoidable light exposure during experimental procedures. DV and MV pigments are differentiated by positions of Soret bands in the absorption spectra. (**E**) Accumulation of GG–Chl a in the DE/IG strain and of Chl a in the DE/BoP/IG strain monitored by absorbance at 665 nm. The production of authentic Chl a was further confirmed by LC-MS with the acquired mass spectrum shown in the inset (see fig. S6 for details). The pigment accumulated in the IG strain was not assigned because of lack of an appropriate pigment standard.

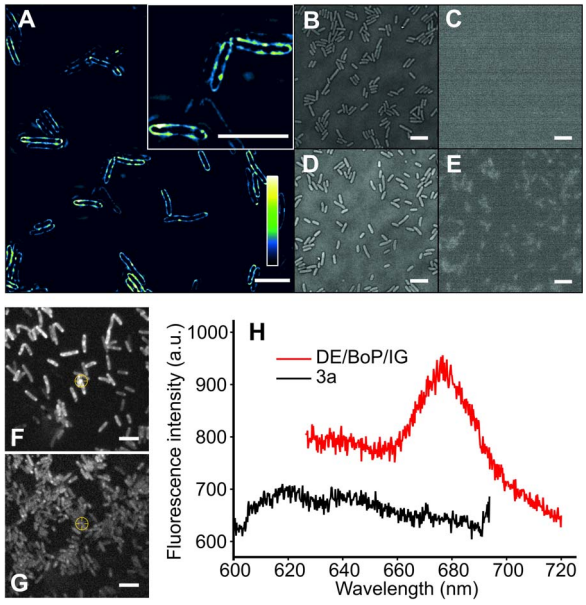

Fig. 4. SIM and fluorescence emission spectroscopy on the cellular distribution of Chl a in *E. coli*. (**A**) SIM of the ALA-fed *E. coli* DE/BoP/IG cells. The color bar shows the color map of the image. The inset image shows the cellular distribution of Chl a in more detail. Scale bars, 5 μm. *E. coli* 3a cells with or without ALA feeding showed zero or limited fluorescence. (**B** to **E**) Bright-field and epifluorescence images of the *E. coli* 3a cells without (B and C) and with ALA feeding (D and E). Scale bars, 5 μm. (**F** and **G**) Fluorescence images of the ALA-fed *E. coli* (F) DE/BoP/IG and (G) 3a cells immobilized on an agar gel pad. Scale bars, 5 μm. (**H**) Fluorescence emission spectra recorded from individual *E. coli* DE/BoP/IG cells [marked with a front sight symbol in (G)]. a.u., arbitrary units.

cyclase step that confers the green color to Chl, we have been able to assemble a cyclase gene, together with 11 others, to form a Chl biosynthetic pathway in *E. coli*. The PPIX substrate for this new pathway is furnished by the host's tetrapyrrole metabolism, and the widespread availability of PPIX in most forms of life could provide the basis for installing Chl biosynthesis in a variety of heterotrophic organisms. This work forms the basis for performing in vitro cyclase assays with defined components and will enable molecular biologists to reprogram the cellular energetics of various platform organisms to include solar energy capture, commencing a new era of light-powered synthetic biology.

MATERIALS AND METHODS

Bacterial strains and plasmids

Bacterial strains and plasmids used in this study are listed in table S2. Primers used for plasmid construction and screening mutants are listed in table S3. *E. coli* strains were grown in LB medium at 37°C. If required, antibiotics were added at 30 μg ml^{-1} for kanamycin, 100 μg ml^{-1} for ampicillin, and 34 μg ml^{-1} for chloramphenicol. *Rvi. gelatinosus* strains were grown in polypeptone-yeast extract-sodium succinate (PYS) medium (*30*) at 30°C. *Synechocystis* strains were grown in blue-green 11 (BG-11) medium (*31*) buffered with 10 mM *N*-tris(hydroxymethyl)methyl-2-aminoethanesulfonic acid (pH 8.3, adjusted by KOH) at 30°C with continuous illumination. Glucose was added at 5 mM if required. The *Rba. capsulatus* strain (SB1003) (*32*), resistant to rifampicin, was obtained from C. Bauer (Indiana University) and grown in mineral-peptone-yeast extract (MPYE) medium (*33*) at 30°C. If required, antibiotics were added at 30 μg ml^{-1} for kanamycin and 20 μg ml^{-1} for rifampicin.

The allelic exchange suicide vector pK18mobsacB (*34*) was used to construct marker-free in-frame deletion mutant of *Rba. capsulatus*. For construction of the pK18Δ*bchE* plasmid, the upstream and downstream regions (approximately 500 base pairs) of the *bchE* gene were polymerase chain reaction (PCR)–amplified from *Rba. capsulatus* genomic DNA with primers bchEUpXbaIF/bchEUpR and bchEDownF/bchEDownHindIIIR, respectively. The two PCR products were fused by overlap extension PCR, digested with Xba I and Hind III, and ligated into the digested pK18mobsacB vector. The pK18Δ*ccoP* plasmid was constructed in the same manner with the relevant primers. For construction of the pBB[*acsF*] plasmid, two parts of the *acsF* gene were PCR-amplified from *Rvi. gelatinosus* genomic DNA with the acsFBglIIF/acsFremoveBglIIR and acsFremoveBglIIF/acsFNotIR primers. The two PCR products were fused by overlap extension PCR, digested with Bgl II and Not I, and ligated into the digested pBBRBB-$Ppuf_{843–1200}$ vector (*35*). For construction of the DE plasmid, the *crtE* gene was amplified by PCR from *Rvi. gelatinosus* genomic DNA with the crtENdeIF/crtEXhoIR primers, digested with Nde I and Xho I, and ligated into the pCOLADuet1 vector to obtain pCOLADuet1-*crtE*. Three parts of the *E. coli dxs* gene were amplified by PCR from a plasmid containing the gene with the dxsNcoIF/dxsremoveHindIII1R, dxsremoveHindIII1F/dxsremoveHindIII2R, and dxsremoveHindIII2F/dxsHindIIIR primers. The three PCR products were fused by overlap extension PCR, digested with Nco I and Hind III, and ligated into the digested pCOLADuet1-*crtE* to obtain the DE plasmid. For construction of the BoP plasmid, the *chlP* gene was PCR-amplified from *Synechocystis* genomic DNA with chlPNdeIF/chlPXhoIR primers, digested with Nde I and Xho I, and ligated into the digested pACYCDuet1 vector to obtain the pACYCDuet1-*chlP* plasmid. The sequence encoding the BoWSCP-His_{10} was cut from the pIND4[WSCP] plasmid (*10*) using Nco I and Hind III and ligated into the digested pACYCDuet1-*chlP* to obtain the BoP plasmid.

The *Synechocystis chlI*, *chlD*, and *chlH* genes were subcloned from the pET9a-SynI, pET9a-SynD, and pET9a-SynH plasmids (*36*), respectively. The Hind III and Xba I sites in the *chlI* gene were removed by site-directed mutagenesis with the chlIremoveHindIIIF/chlIremoveHindIIIR and chlIremoveXbaIF/chlIremoveXbaIR primers. An Spe I site was introduced to pET9a-SynI (Hind III and Xba I sites removed), pET9a-SynD, and pET9a-SynH by site-directed mutagenesis with the primers pETaddSpeIF/pETaddSpeIR. Then, the *chlI*, *chlD*, and *chlH* genes were excised from the pET9a constructs with Nde I and Spe I and ligated into the Spe I–digested pET3a vector. The *Synechocystis gun4* gene was PCR-amplified from *Synechocystis* genomic DNA with the gun4NdeIF/gun4SpeIR primers, digested with Nde I and Spe I, and ligated into the digested Spe I–added pET3a vector. Then, the Hind III and Xba I sites in the *gun4* gene were removed by site-directed mutagenesis with the gun4removeHindIIIF/gun4removeHindIIIR and gun4removeXbaIF/gun4removeXbaIR primers. The *Synechocystis chlM*, *por*, *dvr*, *chlG*, *chlP*, *cycI*, and *ycf54* genes were PCR-amplified from *Synechocystis* genomic DNA with the relevant geneNdeIF/geneSpeIBamHIR primers, digested with Nde I and BamH I, and ligated into the digested pET3a vector. The Hind III site in the *por* gene and the Spe I site in the *dvr* gene were subsequently removed by site-directed mutagenesis with the porremoveHindIIIF/porremoveHindIIIR and dvrremoveSpeIF/dvrremoveSpeIR primers, respectively. The *acsF* gene was PCR-amplified from *Rvi. gelatinosus* genomic DNA with the acsFNdeIF/acsFSpeIBamHIR primers, digested with Nde I and BamH I, and ligated into the digested pET3a vector. Then, genes were cut from the pET3a constructs and adjoined one by one in the described order using the link-and-lock method, as depicted in fig. S2. Plasmids were sequenced by GATC Biotech.

Construction and phenotypic analysis of *Rba. capsulatus* mutants

The deletion plasmids pK18Δ*bchE* and pK18Δ*bchE* were transformed into the *E. coli* S17-1 strain (*37*), and transformants were selected on LB agar with kanamycin (30 μg ml^{-1}). A single colony from the plate was inoculated to 5 ml of LB medium with kanamycin (30 μg ml^{-1}) and grown at 37°C for 24 hours. *E. coli* cells harvested from 3 ml of the culture were resuspended in 50 μl of LB medium and mixed with *Rba. capsulatus* cells, which were harvested from 30 ml of liquid culture and resuspended in 100 μl of LB medium. The mating mixture was spotted onto solid LB medium and incubated at 30°C overnight. The mixture was streaked out onto MPYE agar supplemented with kanamycin (30 μg ml^{-1}) and rifampicin (20 μg ml^{-1}). The obtained kanamycin-resistant transconjugants were subcultured three times in nonselective MPYE medium to allow a second homologous recombination. Then, the culture was diluted and spread onto MPYE agar with 10% (w/v) sucrose. Colonies were then replica-plated onto MPYE plates containing 10% (w/v) sucrose, containing and lacking kanamycin (30 μg ml^{-1}). The desired mutants were screened from the kanamycin-sensitive and sucrose-resistant colonies by PCR with the geneScreenF/geneScreenR primers. The expression plasmid pBB[*acsF*] was conjugated into *Rba. capsulatus* via *E. coli* S17-1 using the same method as described above. Transconjugants harboring the plasmid were selected on MPYE agar with kanamycin (30 μg ml^{-1}) and rifampicin (20 μg ml^{-1}).

For phenotypic analysis, *Rba. capsulatus* strains were grown in 10 ml of MPYE medium in 50-ml Falcon tubes with shaking at 230 rpm. Cells were harvested and resuspended in 1 ml of 60% (w/v) sucrose before recording absorption spectra of whole cells. Pigments were extracted from cells standardized by OD_{680} with methanol. The absorption spectra of whole cells and pigment extracts were recorded on a Cary 60 UV-Vis spectrophotometer, whereas those for whole cells were normalized and corrected for light scattering, as described previously (*38*).

In vivo enzymatic assay of cyclase in *E. coli*

E. coli C43(DE3) was transformed with either the pET3a or the pET3a-*acsF* plasmid and selected on LB agar with ampicillin (100 μg ml^{-1}). For in vivo assays, a single colony was used to inoculate 10 ml of LB medium with ampicillin (100 μg ml^{-1}) and grown overnight at 37°C, with shaking at 220 rpm. The next day, 30 to 50 μl of the resulting culture were used to inoculate 10 ml of LB medium with ampicillin (100 μg ml^{-1}) and grown as above until the OD_{600} reached 0.4 to 0.6. IPTG was added at 0.5 mM to induce gene expression. Meanwhile, purified MgPME dissolved in methanol was directly added to cultures. The cultures were incubated for a further 24 hours at 30°C, with shaking at 175 rpm, before pigments were extracted from the cells.

Synthetic production of Chl a in *E. coli*

E. coli C43(DE3) was transformed with the pET3a-based plasmids containing Chl biosynthesis genes and selected on LB agar with ampicillin (100 μg ml^{-1}). For the DE/IG strain, two sequential transformations were conducted, and the second transformation was selected on LB agar with ampicillin (100 μg ml^{-1}) and kanamycin (30 μg ml^{-1}). For the DE/BoP/IG strain, three sequential transformations were conducted, and the third transformation was selected on LB agar with ampicillin (100 μg ml^{-1}), kanamycin (30 μg ml^{-1}), and chloramphenicol (34 μg ml^{-1}). A single colony was used to inoculate liquid medium and cultured as above, except that, at the point of induction, ALA and Mg^{2+} (equimolar mixture of $MgCl_2$ and $MgSO_4$) were also added at 10 mM. Cultures requiring light activation were illuminated with 5 μmol photons m^{-2} s^{-1} light for the final 4 hours.

Pigment extraction

E. coli cells were harvested from liquid cultures and washed in 25 mM Hepes buffer (pH 7.4). Pigments were extracted with an excess of methanol by vigorous shaking using a Mini-Beadbeater (BioSpec), incubated on ice for 10 min, and centrifuged at 16,000*g* for 5 min at 4°C. The resulting supernatant containing extracted pigments was transferred to a new tube and analyzed immediately or vacuum-dried at 30°C using a Concentrator plus (Eppendorf) and stored at −20°C for future analysis. GG–Chl a was extracted from a *Synechocystis* Δ*chlP* mutant (*10*) using the same method as described above. MgPME was extracted from a *Rvi. gelatinosus* Δ*bchE*Δ*acsF* mutant (*5*), which excreted the pigment into the growth medium as granules. Cells were harvested from liquid culture and washed in ultrapure water, and the pellet was suspended in methanol with gentle shaking to facilitate dissolution of the pigment into the solvent. MgPME solution was collected from the colored supernatant after centrifugation at 5000*g* at 4°C for 10 min.

High-performance liquid chromatography

A methanolic pigment solution, either freshly extracted or reconstituted from dried samples, was analyzed on an Agilent 1200 HPLC system equipped with a diode array detector and a fluorescence detector. A published method (*39*) with some modifications was used for separation of Chl a and its precursors. The pigment solution was loaded onto a Sigma-Aldrich Discovery C18 reversed-phase column (particle size, 5 μm; 250 mm × 4.6 mm). Solvent A was methanol/500 mM ammonium acetate (30/70, v/v). Solvent B was methanol. Pigment species were eluted at 40°C at a flow rate of 1 ml min^{-1} with a linear gradient of 65 to 75% solvent B over 35 min, followed by column wash with 100% solvent B for 15 min. The eluates were monitored by absorbance at 416, 440, and 665 nm.

Liquid chromatography–mass spectrometry

An Agilent 1200 HPLC system coupled to a 6410 QQQ mass spectrometer was used for confirmation of production of authentic Chl a. Data were collected and analyzed with MassHunter Software. Pigments were initially separated by reversed-phase HPLC using an identical program to that described above. The elution of Chl a from the column was monitored by checking absorbance at 665 nm. The assignment of *m/z* to eluates was performed using in-line electrospray ionization in positive mode monitoring *m/z* between 800 and 1000.

Structured illumination microscopy

E. coli cells were pelleted and washed with phosphate-buffered saline and resuspended to an appropriate density for microscopy. Cell suspensions were incubated on an agarose pad for 30 min and mounted in VECTASHIELD Antifade Medium (Vector Laboratories). Samples were imaged on a DeltaVision OMX V4 microscope with the Blaze 3D structured illumination module equipped with a 60× oil objective [numerical aperture (NA), 1.42]. Illumination was performed with a 642-nm laser with the emitted light collected through a 683/40 bandpass filter. For each SIM image, nine axial planes were captured with a spacing of 125 nm, and the data were reconstructed with the SoftWoRx 6.0 software package (GE Healthcare).

Fluorescence spectroscopy

Resuspended frozen *E. coli* cells (20 μl) were spotted onto LB agar and left until the liquid was absorbed into the agar. The cell spot was cut out

of the agar and flipped over onto a glass-bottomed petri dish (WillCo Wells, GWSt-3522). The petri dish was then mounted in the microscope sample holder for imaging. Fluorescence imaging and emission spectral measurements were performed on a home-built imager equipped with a spectrometer (Acton SP2558, Princeton Instruments) and an electron-multiplying charge-coupled device camera (ProEM 512, Princeton Instruments). Dual-sample illumination was provided by a 470-nm light-emitting diode light source (M470L2, ThorLabs) to provide Köhler illumination for wide-field imaging and a 485-nm pulsed laser (LDH-D-C-485, PicoQuant) for a critical illumination when recording the emission spectra of individual cells. The laser beam was focused on the sample surface to a diffraction-limited spot using a 100× objective (PlanFluorite; NA, 1.4; oil immersion, Olympus), illuminating only a portion of the individual cell. Fluorescence signal was filtered through a 495-nm dichroic mirror (FF495-Di03, Semrock) and a 594-nm long-pass filter (BLP01-594R-25, Semrock). The emission spectra were recorded using a diffraction grating of 150 g mm^{-1} with an 800-nm blaze, resulting in a wavelength range of 114 nm. The central wavelength was always selected to match the peak emission wavelength of the sample.

SUPPLEMENTARY MATERIALS

Supplementary material for this article is available at http://advances.sciencemag.org/cgi/content/full/4/1/eaaq1407/DC1

fig. S1. Deletions of the *bchE* and *ccoP* genes in *Rba. capsulatus*.
fig. S2. Diagram of the link-and-lock method for plasmid construction.
fig. S3. The production of DV PChlide a in the IA and IM-*cycI-ycf54* strains.
fig. S4. The light-dependent production of MV Chlide a in the ID strain.
fig. S5. The production of GG–Chl a in the DE/IG strain and of Chl a in the DE/BoP/IG strain.
fig. S6. Verification of the production of Chl a in *E. coli* by LC-MS.
fig. S7. Western blot analysis of the BoWSCP-His_{10} expression in the DE/BoP/IG strain.
table S1. List of genes used to assemble the Chl biosynthesis pathway in *E. coli*.
table S2. Strains and plasmids described in this study.
table S3. Oligonucleotide primers used in this study.

REFERENCES AND NOTES

1. P. Brzezowski, A. S. Richter, B. Grimm, Regulation and function of tetrapyrrole biosynthesis in plants and algae. *Biochim. Biophys. Acta* **1847**, 968–985 (2015).
2. J. W. Chidgey, M. Linhartová, J. Komenda, P. J. Jackson, M. J. Dickman, D. P. Canniffe, P. Koník, J. Pilný, C. N. Hunter, R. Sobotka, A cyanobacterial chlorophyll synthase-HliD complex associates with the Ycf39 protein and the YidC/Alb3 insertase. *Plant Cell* **26**, 1267–1279 (2014).
3. Y. Fujita, H. Yamakawa, Biochemistry of chlorophyll biosynthesis in photosynthetic prokaryotes, in *Modern Topics in the Phototrophic Prokaryotes*, P. Hallenbeck, Ed. (Springer, 2017), pp. 67–122.
4. S. P. Gough, B. O. Petersen, J. Ø. Duus, Anaerobic chlorophyll isocyclic ring formation in *Rhodobacter capsulatus* requires a cobalamin cofactor. *Proc. Natl. Acad. Sci. U.S.A.* **97**, 6908–6913 (2000).
5. G. E. Chen, D. P. Canniffe, C. N. Hunter, Three classes of oxygen-dependent cyclase involved in chlorophyll and bacteriochlorophyll biosynthesis. *Proc. Natl. Acad. Sci. U.S.A.* **114**, 6280–6285 (2017).
6. K. Rzeznicka, C. J. Walker, T. Westergren, C. G. Kannangara, D. von Wettstein, S. Merchant, S. P. Gough, M. Hansson, *Xantha-l* encodes a membrane subunit of the aerobic Mg-protoporphyrin IX monomethyl ester cyclase involved in chlorophyll biosynthesis. *Proc. Natl. Acad. Sci. U.S.A.* **102**, 5886–5891(2005).
7. V. Pinta, M. Picaud, F. Reiss-Husson, C. Astier, *Rubrivivax gelatinosus acsF* (previously *orf358*) codes for a conserved, putative binuclear-iron-cluster-containing protein involved in aerobic oxidative cyclization of Mg-protoporphyrin IX monomethylester. *J. Bacteriol.* **184**, 746–753 (2002).
8. G. E. Chen, D. P. Canniffe, E. C. Martin, C. N. Hunter, Absence of the cbb_3 terminal oxidase reveals an active oxygen-dependent cyclase involved in bacteriochlorophyll biosynthesis in *Rhodobacter sphaeroides*. *J. Bacteriol.* **198**, 2056–2063 (2016).
9. S.-W. Kim, J. D. Keasling, Metabolic engineering of the nonmevalonate isopentenyl diphosphate synthesis pathway in *Escherichia coli* enhances lycopene production. *Biotechnol. Bioeng.* **72**, 408–415 (2001).
10. A. Hitchcock, P. J. Jackson, J. W. Chidgey, M. J. Dickman, C. N. Hunter, D. P. Canniffe, Biosynthesis of chlorophyll *a* in a purple bacterial phototroph and assembly into a plant chlorophyll–protein complex. *ACS Synth. Biol.* **5**, 948–954 (2016).
11. B. Miroux, J. E. Walker, Over-production of proteins in *Escherichia coli*: Mutant hosts that allow synthesis of some membrane proteins and globular proteins at high levels. *J. Mol. Biol.* **260**, 289–298 (1996).
12. K. Minamizaki, T. Mizoguchi, T. Goto, H. Tamiaki, Y. Fujita, Identification of two homologous genes, $chlA_I$ and $chlA_{II}$, that are differentially involved in isocyclic ring formation of chlorophyll *a* in the cyanobacterium *Synechocystis* sp. PCC 6803. *J. Biol. Chem.* **283**, 2684–2692 (2008).
13. E. Peter, A. Salinas, T. Wallner, D. Jeske, D. Dienst, A. Wilde, B. Grimm, Differential requirement of two homologous proteins encoded by *sll1214* and *sll1874* for the reaction of Mg protoporphyrin monomethylester oxidative cyclase under aerobic and micro-oxic growth conditions. *Biochim. Biophys. Acta* 1787, 1458–1467 (2009).
14. S. Hollingshead, J. Kopečná, P. J. Jackson, D. P. Canniffe, P. A. Davison, M. J. Dickman, R. Sobotka, C. N. Hunter, Conserved chloroplast open-reading frame *ycf54* is required for activity of the magnesium protoporphyrin monomethylester oxidative cyclase in *Synechocystis* PCC 6803. *J. Biol. Chem.* **287**, 27823–27833 (2012).
15. S. Hollingshead, J. Kopečná, D. R. Armstrong, L. Bucinska, P. J. Jackson, G. E. Chen, M. J. Dickman, M. P. Williamson, R. Sobotka, C. N. Hunter, Synthesis of chlorophyll-binding proteins in a fully segregated *Δycf54* strain of the cyanobacterium *Synechocystis* PCC 6803. *Front. Plant Sci.* **7**, 292 (2016).
16. W. Rüdiger, J. Benz, C. Guthoff, Detection and partial characterization of activity of chlorophyll synthetase in etioplast membranes. *Eur. J. Biochem.* **109**, 193–200 (1980).
17. M. G. Gustafsson, L. Shao, P. M. Carlton, C. J. R. Wang, I. N. Golubovskaya, W. Z. Cande, D. A. Agard, J. W. Sedat, Three-dimensional resolution doubling in wide-field fluorescence microscopy by structured illumination. *Biophys. J.* **94**, 4957–4970 (2008).
18. H. Satoh, A. Uchida, K. Nakayama, M. Okada, Water-soluble chlorophyll protein in Brassicaceae plants is a stress-induced chlorophyll-binding protein. *Plant Cell Physiol.* **42**, 906–911 (2001).
19. J. Nickelsen, B. Rengstl, Photosystem II assembly: From cyanobacteria to plants. *Annu. Rev. Plant Biol.* **64**, 609–635 (2013).
20. H. Yang, J. Liu, X. Wen, C. Lu, Molecular mechanism of photosystem I assembly in oxygenic organisms. *Biochim. Biophys. Acta* **1847**, 838–848 (2015).
21. J. J. Eaton-Rye, R. Sobotka, Assembly of the photosystem II membrane-protein complex of oxygenic photosynthesis. *Front. Plant Sci.* **8**, 884 (2017).
22. E. Raux, H. K. Leech, R. Beck, H. L. Schubert, P. J. Santander, C. A. Roessner, A. I. Scott, J. H. Martens, D. Jahn, C. Thermes, A. Rambach, M. J. Warren, Identification and functional analysis of enzymes required for precorrin-2 dehydrogenation and metal ion insertion in the biosynthesis of sirohaem and cobalamin in *Bacillus megaterium*. *Biochem. J.* **370**, 505–516 (2003).
23. I. U. Heinemann, M. Jahn, D. Jahn, The biochemistry of heme biosynthesis. *Arch. Biochem. Biophys.* **474**, 238–251 (2008).
24. G. Layer, J. Reichelt, D. Jahn, D. W. Heinz, Structure and function of enzymes in heme biosynthesis. *Protein Sci.* **19**, 1137–1161 (2010).
25. S. I. Beale, Biosynthesis of Open-Chain Tetrapyrroles in Plants, Algae, and Cyanobacteria, in *Ciba Foundation Symposium 180-The Biosynthesis of the Tetrapyrrole Pigments*, D. J. Chadwick, K. Ackrill, Eds. (Wiley, 1994), pp. 156–176.
26. R. M. Alvey, A. Biswas, W. M. Schluchter, D. A. Bryant, Attachment of noncognate chromophores to CpcA of *Synechocystis* sp. PCC 6803 and *Synechococcus* sp. PCC 7002 by heterologous expression in *Escherichia coli*. *Biochemistry* **50**, 4890–4902 (2011).
27. M. J. Warren, E. Raux, H. L. Schubert, J. C. Escalante-Semerena, The biosynthesis of adenosylcobalamin (vitamin B_{12}). *Nat. Prod. Rep.* **19**, 390–412 (2002).
28. K. Zheng, P. D. Ngo, V. L. Owens, X.-P. Yang, S. O. Mansoorabadi, The biosynthetic pathway of coenzyme F430 in methanogenic and methanotrophic archaea. *Science* **354**, 339–342 (2016).
29. S. J. Moore, S. T. Sowa, C. Schuchardt, E. Deery, A. D. Lawrence, J. V. Ramos, S. Billig, C. Birkemeyer, P. T. Chivers, M. J. Howard, S. E. J. Rigby, G. Layer, M. J. Warren, Elucidation of the biosynthesis of the methane catalyst coenzyme F_{430}. *Nature* **543**, 78–82 (2017).
30. K. V. Nagashima, K. Shimada, K. Matsuura, Shortcut of the photosynthetic electron transfer in a mutant lacking the reaction center-bound cytochrome subunit by gene disruption in a purple bacterium, *Rubrivivax gelatinosus*. *FEBS Lett.* **385**, 209–213 (1996).
31. R. Rippka, J. Deruelles, J. B. Waterbury, M. Herdman, R. Y. Stanier, Generic assignments, strain histories and properties of pure cultures of cyanobacteria. *Microbiology* **111**, 1–61 (1979).
32. H.-C. Yen, B. Marrs, Map of genes for carotenoid and bacteriochlorophyll biosynthesis in *Rhodopseudomonas capsulata*. *J. Bacteriol.* **126**, 619–629 (1976).
33. H.-G. Koch, O. Hwang, F. Daldal, Isolation and characterization of *Rhodobacter capsulatus* mutants affected in cytochrome cbb_3 oxidase activity. *J. Bacteriol.* **180**, 969–978 (1998).
34. A. Schäfer, A. Tauch, W. Jäger, J. Kalinowski, G. Thierbach, A. Pühler, Small mobilizable multi-purpose cloning vectors derived from the *Escherichia coli* plasmids pK18 and pK19: Selection of defined deletions in the chromosome of *Corynebacterium glutamicum*. *Gene* **145**, 69–73 (1994).

35. I. B. Tikh, M. Held, C. Schmidt-Dannert, BioBrick™ compatible vector system for protein expression in *Rhodobacter sphaeroides*. *Appl. Microbiol. Biotechnol.* **98**, 3111–3119 (2014).
36. P. E. Jensen, L. C. Gibson, K. W. Henningsen, C. N. Hunter, Expression of the *chlI*, *chlD*, and *chlH* genes from the cyanobacterium *Synechocystis* PCC6803 in *Escherichia coli* and demonstration that the three cognate proteins are required for magnesium-protoporphyrin chelatase activity. *J. Biol. Chem.* **271**, 16662–16667 (1996).
37. R. Simon, U. Priefer, A. Pühler, A broad host range mobilization system for in vivo genetic engineering: Transposon mutagenesis in gram negative bacteria. *Nat. Biotechnol.* **1**, 784–791 (1983).
38. D. J. Swainsbury, S. Scheidelaar, R. van Grondelle, J. A. Killian, M. R. Jones, Bacterial reaction centers purified with styrene maleic acid copolymer retain native membrane functional properties and display enhanced stability. *Angew. Chem. Int. Ed.* **53**, 11803–11807 (2014).
39. R. Sobotka, M. Tichy, A. Wilde, C. N. Hunter, Functional assignments for the carboxyl-terminal domains of the ferrochelatase from *Synechocystis* PCC 6803: The CAB domain plays a regulatory role, and region II is essential for catalysis. *Plant Physiol.* **155**, 1735–1747 (2011).
40. H. M. McGoldrick, C. A. Roessner, E. Raux, A. D. Lawrence, K. J. McLean, A. W. Munro, S. Santabarbara, S. E. J. Rigby, P. Heathcote, A. I. Scott, M. J. Warren, Identification and characterization of a novel vitamin B_{12} (cobalamin) biosynthetic enzyme (CobZ) from *Rhodobacter capsulatus*, containing flavin, heme, and Fe-S cofactors. *J. Biol. Chem.* **280**, 1086–1094 (2005).

Acknowledgments: We thank C. Bauer (Indiana University) for the gift of the *Rba. capsulatus* SB1003 strain, M. Proctor for providing the DV PChlide a and DV Chlide a standards, A. Hitchcock for providing the Chl a standard, and M. Radle (Pennsylvania State University) for assistance with LC-MS data collection. **Funding:** C.N.H. acknowledges financial support from Advanced Award 338895 from the European Research Council. C.N.H., G.E.C., and A.A.B. acknowledge funding from the Biotechnology and Biological Sciences Research Council (award number BB/M000265/1). D.P.C. is supported by the European Commission (Marie Skłodowska-Curie Global Fellowship 660652). S.F.H.B. was supported by a University of Sheffield 2022 Futures Studentship. D.A.B. acknowledges funding by NSF grant MCB-1613022 and Division of Chemical Sciences, Geosciences, and Biosciences, Office of Basic Energy Sciences of the U.S. Department of Energy (DOE) grant DE-FG02-94ER20137. Research in the laboratories of C.N.H. and D.A.B. was also conducted under the auspices of the Photosynthetic Antenna Research Center, an Energy Frontier Research Center funded by the DOE, Office of Science, Office of Basic Energy Sciences under award number DE-SC 0001035. The SIM imaging was performed at the University of Sheffield Wolfson Light Microscopy Facility and was partly funded by Medical Research Council grant MR/K015753/1. S.H. was supported by a doctoral studentship from the University of Sheffield. **Author contributions:** G.E.C., S.H., and A.A.B. made the plasmid constructs. G.E.C. made the *Rba. capsulatus* mutants and conducted in vivo *E. coli* assays and pigment analyses. D.P.C. provided the LC-MS data and contributed ideas concerning interpretation of the data and the manuscript. S.F.H.B. provided the SIM data. C.V. provided the fluorescence emission spectroscopy data. D.A.B. contributed ideas concerning experimental evidence, the manuscript, and support for D.P.C. G.E.C. and C.N.H. designed the experiments, interpreted the data, and wrote the manuscript. **Competing interests:** The authors declare that they have no competing interests. **Data and materials availability:** All data needed to evaluate the conclusions in the paper are present in the paper and/or the Supplementary Materials. Additional data related to this paper may be requested from the authors.

Submitted 5 October 2017
Accepted 28 December 2017
Published 26 January 2018
10.1126/sciadv.aaq1407

Citation: G. E. Chen, D. P. Canniffe, S. F. H. Barnett, S. Hollingshead, A. A. Brindley, C. Vasilev, D. A. Bryant, C. N. Hunter, Complete enzyme set for chlorophyll biosynthesis in *Escherichia coli*. *Sci. Adv.* **4**, eaaq1407 (2018).